# RManuscript 23.01.2023.docx

**Abstract**

**Background**: Prostate cancer (PCa) remains one of the clinically relevant pathologies that needs pragmatic and effective treatment approaches with limited side effects. The current study aimed to evaluate the anticancer potential of epigallocatechin gallate (EGCG) and EGCG-loaded nanoparticles (EGCG NP) for the treatment of prostate cancer in in-vitro 3D spheroid model. **Methods**: The EGCG NPs was synthesized by using polymeric method as reported in our previous study. A 3D spheroid assay was conducted using human prostate specific cell lines (PC3 and 22Rv1) cultured on poly-HEMA-covered plates at different time points. Once formed, the spheroids were treated with either EGCG alone or with EGCG NPs continuously for 6 days. Simultaneously, specific controls were also taken for comparison purpose. CellROX dye was used to quantitate the formation of reactive oxygen species (ROS) in response to EGCG and EGCG NPs to 22Rv1 and PC3, 3D spheroids. The treated spheroids were also evaluated to measure modulation in mitochondrial membrane potential and the quantification of apoptotic and live cells using a flow cytometer. **Results**: The spheroid sizes of both studied cell lines were found to be significantly ($p < 0.05$) reduced after the treatment with EGCG and its nanoformulation. The significant increase in ROS formation was observed in PC3 cells in response to EGCG and EGCG-NPs treatment. However, no significant change in ROS formation was observed in 22Rv1 cells. Similarly, both compounds (EGCG and EGCG NPs) did not show any significant changes in mitochondrial membrane potential in 22Rv1 and PC3 spheroids. Interestingly, EGCG treatment showed a significant change between live and apoptotic cells in both 22Rv1 and PC3 spheroids but its nanoformulation didn't show significant change in the number of apoptotic and live cells. Our study observed a significant anticancer potential of EGCG and EGCG NPs at clinically relevant doses highlighting the possible advantage of 3D spheroid model specifically in our studied cancer cells. However, further preclinical in vivo studies are recommended in a suitable model to decipher our in vitro data and exploit EGCG and EGCG NPs against prostate cancer.

**Conclusion**: Our results indicate the anticancer efficacy of EGCG and EGCG NPs in 3D spheroids of PCa cell lines.


**Keywords**: 3D spheroids, anticancer, epigallocatechin gallate, nanoparticles, polyphenols, prostate cancer

## Introduction

Prostate cancer (PCa) is one of the clinically relevant pathologies, has progressively increased its global prevalence over the past decade (Li et al., 2022). It is the most often diagnosed male cancer and the leading cause of cancer-associated mortality in males around the globe (Sung et al., 2021). In 2021, it was estimated that 26% of newly found non-cutaneous cancer will be because of prostate cancer resulting in total 11% cancer-related deaths in the USA (Picot et al., 2022). Over the past few years, the incidence of metastatic PCa has increased in all races and age groups, ultimately affecting the survival rate (Sayegh et al., 2022). The existing curative and noncurative therapeutic options of PCa, such as surgery, radiation therapy, hormonal therapy, and chemotherapy are overburdened by various side effects, that include limited clinical efficacy, high cost, and low patient acceptance (Li et al., 2022). In addition, the chemotherapeutic option against PCa is limited due to poor solubility, toxicity, lack of target specificity, nonspecific cell damage and drug resistance (El-Didamony et al., 2022). Despite of the intriguing therapeutic options, the search for pragmatic and more effective treatments modalities that could mitigate above-mentioned undesirable effects are need of the hour.

The surge of naturally derived chemotherapeutic agents provide hopes for effective chemotherapy against PCa (El-Didamony et al., 2022). The phytochemicals have been explored as the cornerstone of highly efficient, well-tolerated, safe, and economical approaches in multifaceted PCa prevention and management (Mazurakova et al., 2022). Based on our earlier research, we also proposed some bioactive molecules and their nanoformulations as potential anticancer agents (Jabir et al., 2012, Tabrez et al., 2013, Jabir et al., 2018, Oves et al., 2018).

Epigallocatechin gallate (EGCG), the primary flavonoid in green tea, has shown significant efficacy in the treatment of cancer due to its considerable therapeutic properties, such as safety, affordability, and bioavailability (Jabir et al., 2018). Several studies suggested that EGCG may inhibit carcinogenesis *via* anti-matrix metalloproteinase and anti-angiogenesis activities, blocking key signal transduction pathways and activating redox-sensitive transcription factors (Liu et al., 2019, Ferrari et al., 2022). The EGCG mediated therapeutic approach needs further improvements in terms of stability, specificity, low absorption, bioavailability, and safety (Dai et al., 2020). In this context, nanotechnology-based approaches have shown significant improvement in anti-cancer potential of EGCG against various cancers (Ahmad et al., 2019, Alserihi et al., 2022). Polymeric nanoparticle is one of the most effective ways to circumvent the delivery and protect

the molecules against undesirable circumstances (Ahmad et al., 2020, Ahmad et al., 2021). Recently, we reported the enhanced antitumor efficacy of EGCG loaded folate receptor-targeted nanoparticles to PCa cells (Alserihi et al., 2022). The current study aimed to assess the therapeutic potential EGCG and EGCG-NPs against PCa cancer cell lines using 3D spheroid model. The purpose of choosing 3D cell culture was to mimic the *in vivo* environment so that we can achieve a robust and more reliable data (Choi et al., 2021).

**Materials and methods**

**Synthesis and characterization of EGCG-NPs**

The polymeric synthesis and characterization of EGCG-NPs using a modified polymeric nanoprecipitation method was described earlier in detail (Alserihi et al., 2022). After dilution of samples with Milli-Q water, NPs' mean diameter and polydispersity index (PDI) were evaluated using photon correlation spectroscopy (Zetasizer Nano ZS, Malvern Instruments, UK) at 25°C and at a scattering angle of 90°. The drug loading content, encapsulation efficiency, and production yields were also evaluated as described (Alserihi et al., 2022).

**Culture of cells**

22Rv1 and PC3, prostate tumorigenic cell lines were procured from ATCC (Manassas, VA, USA). Both cell lines were cultivated in an appropriate culture medium [RPMI-1640 (Gibco, ThermoFisher, USA) and DMEM-high glucose], which included 10% fetal bovine serum and 1% penicillin.

**3D spheroid assay**

For the induction of 3D spheroid, we grew both cancer cell lines on poly-HEMA-coated plates for different time points. Once formed, the spheroids were treated with either EGCG or with EGCG-NPs, continuously for 6 days. Simultaneously, specific control was also taken for comparison purpose. In addition, an empty NPs without EGCG was used as control to compare the effect of EGCG NPs. Every two days, new media was added to replace the spent media. Nikon's inverted light microscope was used to take the spheroids' photos, which were then examined for size using the image J software (https://image j.net/Invasion assay).

**Measurement of reactive oxygen species in spheroids**

Reactive oxygen species (ROS) production in spheroids was measured using the CellROX dye (Life Technologies, Carlsbad, CA, USA). Both cell lines were plated in six-well poly-HEMA-coated plates and continuously exposed to either solvent, EGCG, empty NP, or EGCG NP for 6

days to quantify ROS. CellROX (500 nM) was added when the time point was reached, and it was then incubated at 37°C with 5% $CO_2$ for 60 min. Following the incubation, the samples were examined at flow cytometer utilizing CellROX® Green at 488 nm excitation.

**Measurement of mitochondrial membrane potential in spheroids**

The spheroids were continuously incubated for 6 days with either control and EGCG or empty NP and EGCG NP for the mitochondrial membrane potential (MMP) measurement (Mittal et al., 2017). A flow cytometer (Guava easyCyte™ Luminex) equipped with a 485 nm excitation filter and a 590 nm emission filter was used to examine the treated cells for red and green fluorescence.

**Live/dead assay in spheroids**

Spheroids were continually exposed to solvent, EGCG, empty NP, and EGCG NP for 6 days as part of this test. Propidium iodide (PI) dye in culture media was added to the spheroids once the time point was complete, and they were then washed with 1X PBS and incubated for 10 min at 37°C. A flow cytometer (Guava easyCyteTM Luminex) was then used to examine the cells for red fluorescence.

**Statistical analysis**

The GraphPad Prism 8.0 software was used to conduct a one-way analysis of variance for various groups to find differences between the control and treated groups (GraphPad Software, La Jolla, CA, USA). All the experiments were performed in triplicate and results are reported as mean ± SD. $p < 0.05$ were deemed statistically significant.

**Results and Discussion**

The NPs' particle sizes suggests that the addition of EGCG, did not resulted a significant increase in size when compared to the corresponding free counterparts (Table 1). The 0.12 PDI values that defined the NP dispersions showed a narrow and unimodal distribution, which is typical behavior of monodispersed systems. The encapsulation efficiency of EGCG-NP was found to be 44%, indicating a moderate affinity of the polymeric blend with the EGCG molecules in terms of drug entrapment efficiencies. Additionally, the yields of production were found to be in between 67% and 73%.

Anticancer screening of compounds is mostly performed in conventional 2D cell cultures which often doesn't concur in animal model. Hence, 3D spheroid culture models are gaining interest lately that mimics human tumor tissue conditions (Hundsberger et al., 2021). 3D culture methods typically use an extracellular matrix which imitate tissue key interactions including, cell-to-cell

4

and cell-to-extracellular matrix interactions (Białkowska et al., 2020). In 3D culture, the cells grow, aggregate, and self-assemble in a 3D plane in an environment that prevents attachment to a flat surface, resulting in the formation of spheroid, resembling to *in vivo* tumors (Lazzari et al., 2017). The advantages of 3D spheroids include the possibility of screening a large number of molecules and reducing high cost and ethical issues associated with animal usage (Pinto et al., 2020). In the present study, we used 3D model to assess the impact of both EGCG and EGCG NP treatment in PCa cell lines, namely, 22Rv1 and PC3.

Contemplating the earlier studies, we speculated the diverse therapeutic functions of EGCG in different PCa cell lines could be mediated by androgen sensitivity (Bosutti et al., 2016, Russo et al., 2020). Hence, we choose two different PCa cell lines viz. 22RV1 (androgen-responsive) and PC3 (androgen-nonresponsive) for comparison.

**EGCG and EGCG NPs treatment reduces spheroid size of PCa cell lines**

Spheroid size is one of the crucial aspects to assess the efficacy of the test compounds. The spheroid formation was accomplished by seeding cell suspensions into ultra-low attachment plates. The microscopic examination of these spheroids showed different morphometric characteristics of 22Rv1 and PC3 cells. The treatment of 3D spheroid with the EGCG and EGCG NPs resulted visible changes in their morphology during the treatment period of 6 days. The treatment of EGCG and EGCG NPs showed significant reduction in spheroid size compared to that of control (Figure 1 and Figure 2).

As shown in Figure 1 (a and b upper panel), detachment of both 22Rv1 and PC3 cells resulted in gradual increase of spheroid size in controls, i.e., from 271.5 mm$^3$ on the second day to 569.3 mm$^3$ on the sixth day in 22Rv1 cells and from 243.5 mm$^3$ on the second day to 360.7 mm$^3$ on the sixth day in PC3 cells. EGCG treatment significantly reduces the spheroid sizes on 6$^{th}$ days from 569.3 to 107.9 mm$^3$ (Approximately 130% decline) in the 22Rv1 cell line (Figure 1a, lower panel). Furthermore, we observed a similar decrease in the spheroid size on 6$^{th}$ day from 360.7 to 42.7 mm$^3$ (Approximately 150% decline) in the PC3 cells (Figure 1b, lower panel). Overall, the data clearly showed that the treatment of EGCG significantly attenuates spheroid size of 22Rv1 and PC3 cells.
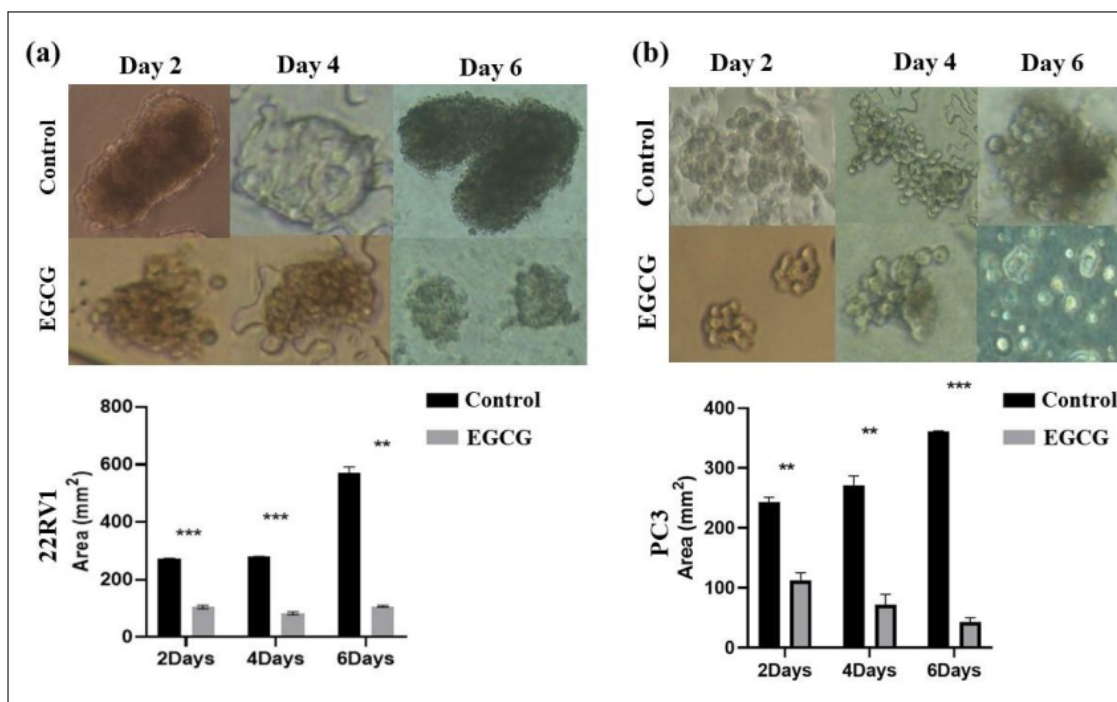
**Figure 1:** Spheroid size decreased with EGCG treatment. Both (a) 22Rv1 and (b) PC3 underwent EGCG treatment for 2–6 days after completing full growth in poly-HEMA-coated plates forming 3D spheroids. Images were captured with a Nikon 40 inverted light microscope, and size analysis was performed using the image J software (mean ± SEM). **P < 0.01, and ***P < 0.001. For size measurement, 100 spheroids in total were examined.

Similarly, we also assessed the impact of EGCG NPs treatment on spheroids size by comparing with empty NPs in 22Rv1 and PC3 cells. As shown in Figure 2 (a and b upper panel), detachment of both cell lines resulted in a gradual increase in spheroid size in the presence of empty NPs, i.e., from 193 mm$^3$ on the second day to 248.3 mm$^3$ on the sixth day in 22Rv1 cells and from 221.2 mm$^3$ on the second day to 348.7 mm$^3$ on the sixth day in PC3 cells. The treatment with EGCG NPs significantly reduces the spheroid sizes on 2$^{nd}$ and 6$^{th}$ days, corresponding to 193 to 95.7 mm$^3$ and 248.3 to 102 mm$^3$, respectively in the 22Rv1 cell line (Figure 2a, lower panel). Albeit there was a decrease in the spheroid size from 222.5 to 131.33 mm$^3$ on the 4$^{th}$ day in 22Rv1, the difference was not statistically significant. Furthermore, we observed a similar decline in the spheroid size on the second day from 221.2 to 114.2 mm$^3$ and 348.7 to 75.6 mm$^3$ on the sixth day

(Figure 2b, lower panel) in the PC3 cell line. Like 22Rv1, PC3 cells also showed a non-significant decrease in spheroid size on the 4$^{th}$ day of EGCG NP treatment from 264.5 to 163.5 mm$^3$. These data revealed that the treatment of EGCG NPs significantly attenuates spheroid formation of detached PCa cells.
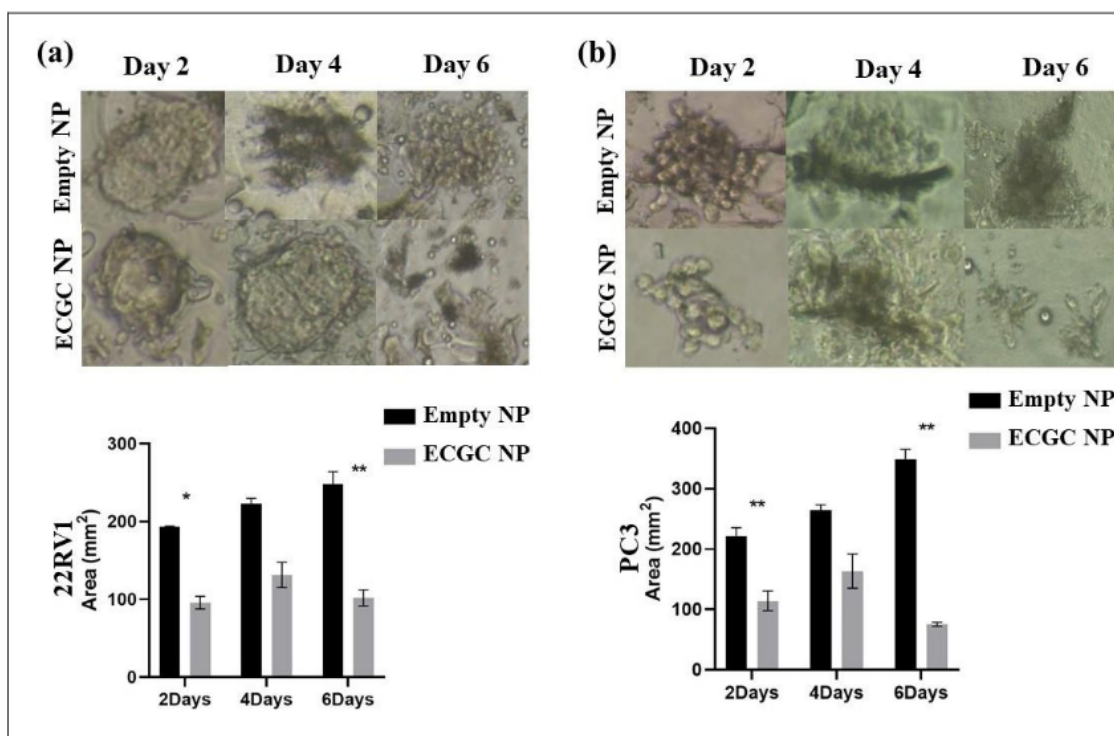


**Figure 2:** Spheroid size is decreased by EGCG NPs treatment. In poly-HEMA-coated plates, (a) 22Rv1 and (b) PC3 were fully grown to form 3D spheroids. Pictures were acquired using a Nikon inverted light microscope at 40x magnification after the spheroids were treated for 2–6 days with empty nanoparticles or EGCG NPs. Using image J software, images were processed for size measurement (mean ± S.E.M.). *P < 0.05, and **P < 0.01. 100 spheroids in total were measured for size analysis.

Spheroid growth result in the formation of necrotic/hypoxic cores with the outside layer largely proliferative, the middle layer hypoxic, and the inner core necrotic (Sims et al., 2017). The efficacy of a drug/compound to penetrate a tumor depends heavily on the size of the tumor because larger tumors exhibit higher resistance, which is also seen in 3D tumor spheroid models (Perez et al., 2021). In the current study, we observed a dramatic decrease in the spheroid size as a result of both EGCG and EGCG NP treatment in 22Rv1 and PC3 cell lines. A comparatively higher reduction

in spheroid size was noted in the PC3 cells after the treatment with EGCG and EGCG NPs. Previous studies suggested various anticancer mechanisms of EGCG and EGCG NPs, such as influence on cellular apoptosis, ROS generation, and inhibition of mutant p53 or tyrosine kinase (Cheng et al., 2020, Farooqi et al., 2020). Our results are concurrent with different studies that uses PLGA/lipid NPs loaded EGCG in 3D models (Hung et al., 2016, Sims et al., 2017, Michy et al., 2019). Sims et al. (2017) reported an increased penetration and distribution of PLGA-modified NPs in HeLa and SiHa spheroids (Sims et al., 2017). The PLGA-encapsulated EtNBS NPs deeply penetrated the 3D spheroid of gastrointestinal carcinoma's hypoxic and acidic cores, which are typically therapeutically resistant tumor regions (Hung et al., 2016). In ovarian spheroid cancer cells, verteporfin-encapsulated lipid nanocarriers effectively inhibited proliferation than free verteporfin (Michy et al., 2019). Similarly, biotin-conjugated pullulan acetate NPs has been noted for comparable anticancer activity in 3D culture and a xenograft hepatic tumor model (Chen et al., 2019).

**EGCG and EGCG NPs treatment induce ROS in spheroids of PC3 not in 22Rv1**

We assessed the impact of control and treatment groups (EGCG & EGCG NPs) on ROS production using flowcytometry by applying CellROX dye at the end of the sixth day in darkness for 30 minutes. The EGCG and EGCG NPs treatment fails to induce a statistically significant production of ROS in 22Rv1 spheroids compared to controls [Figure 3 & 4 (a, upper and lower panels)]. However, EGCG and EGCG NPs treatment induces significant production of ROS in PC3 cells [Figure 3 & 4 (b, upper and lower panels)].

These results indicate involvement of ROS-mediated mechanism(s) in PC3 cells for antitumorigenic effects of EGCG and EGCG NPs. Since, the elevated levels of ROS has been reported to trigger anticancer mechanisms, treating cancer cells with ROS stimulating agents may offer cancer-specific therapy (Gul et al., 2022). The expression of prostate specific membrane antigen (PSMA) have shown relationship with androgen signaling that could play an important clinical implications for PCa treatment (Batra et al., 2019). However, several studies reported that ROS are not an obligatory contributor to produce anticancer effects (Ivanova et al., 2016, Alserihi et al., 2022).
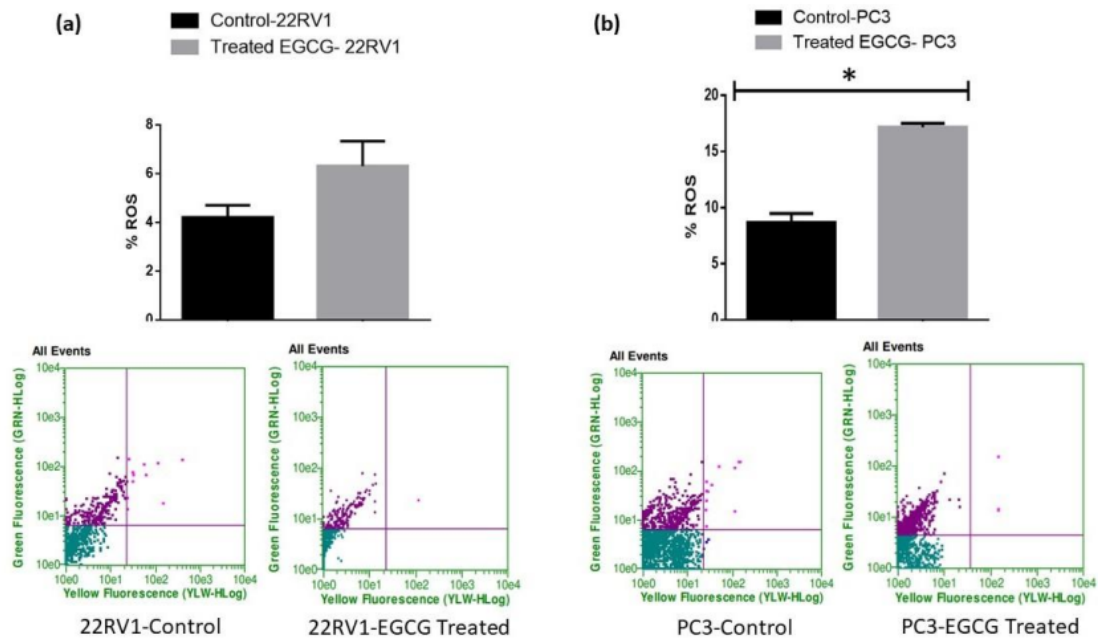
**Figure 3:** EGCG fails to induce ROS in spheroids in 22Rv1 cells (a) and induces ROS in PC-3 cells (b). On poly-HEMA-coated plates, the cells were cultivated before treatment for six days with control or EGCG (6 $\mu$M). CellROX dye was applied to the spheroids at the end of the time point and was incubated for 30 minutes in the dark. The manufacturer-provided standardized wavelength and the Guava Flow Cytometer was used to quantify fluorescent intensity. The values are presented as mean ± SEM (n = 6).
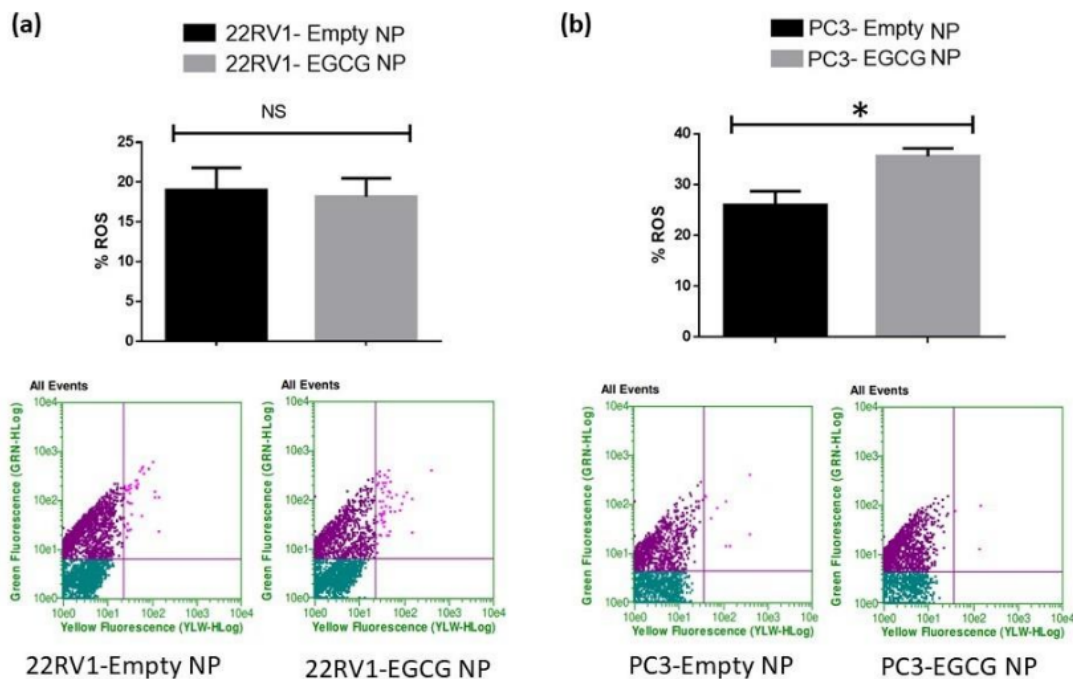
**Figure 4:** EGCG NPs fails to induce ROS in spheroids 22Rv1 cells (a) and induces ROS in PC-3 cells (b). On poly-HEMA-coated plates, the cells were cultivated before being treated for six days with control or EGCG NPs ($6\,\mu$M). CellROX dye was applied to the spheroids at the end of the time point and was incubated for 30 minutes in the dark. The manufacturer-provided standardized wavelength and the Guava Flow Cytometer was used to quantify fluorescent intensity. The values are presented as mean $\pm$ SEM (n = 6).

**EGCG and EGCG NPs treatment fails to promote mitochondrial leakage in PCa cells**

The spheroids of both 22Rv1 and PC3 cells treated with EGCG and EGCG NPs showed a non-significant association in mitochondrial depolarization as evident by JC-1 dye fluorescence (Figure 5 & 6, upper and lower panels). The increase in depolarization and decrease in polarization of mitochondria membrane potential has been reported as important hallmarks of tumorigenesis (Porporato et al., 2018). These results pointed the possibility of mitochondrial independent mechanism of cytotoxicity and ROS production. Recently, Adamczuk et al. (2021) also reported a mitochondria-independent cytotoxic effect of leflunomide in RPMI-8226 multiple myeloma cell lines (Adamczuk et al., 2021). ROS are not only produced by mitochondria in living things, but also by NADPH oxidases, xanthine oxidase, oxidases of aldehydes, amino acids, and carbohydrates under specific conditions in a precise spatiotemporal manner (Lushchak 2016).
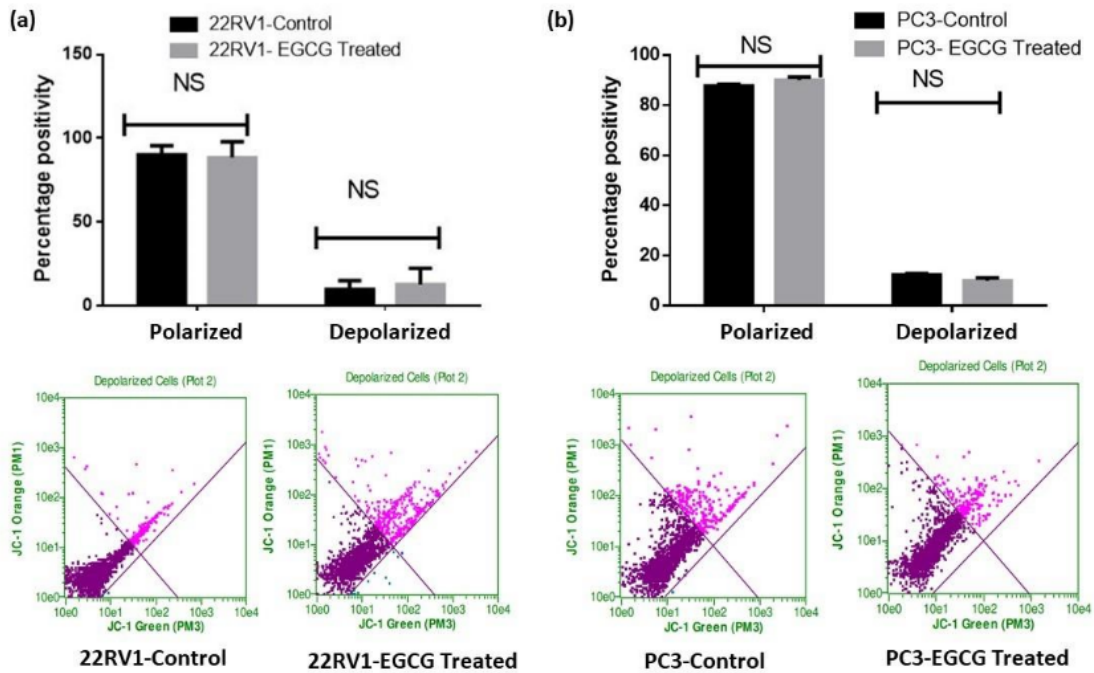
**Figure 5:** EGCG fails to induce depolarization in PCa spheroids. The treated spheroids were mixed with JC-1 dye at the time point's end, and they were then incubated for 30 minutes at 37°C. The manufacturer-provided standardized wavelength for the Guava Flow Cytometer was used to measure the fluorescent intensity. The values are shown as the mean ± SEM (n = 6).
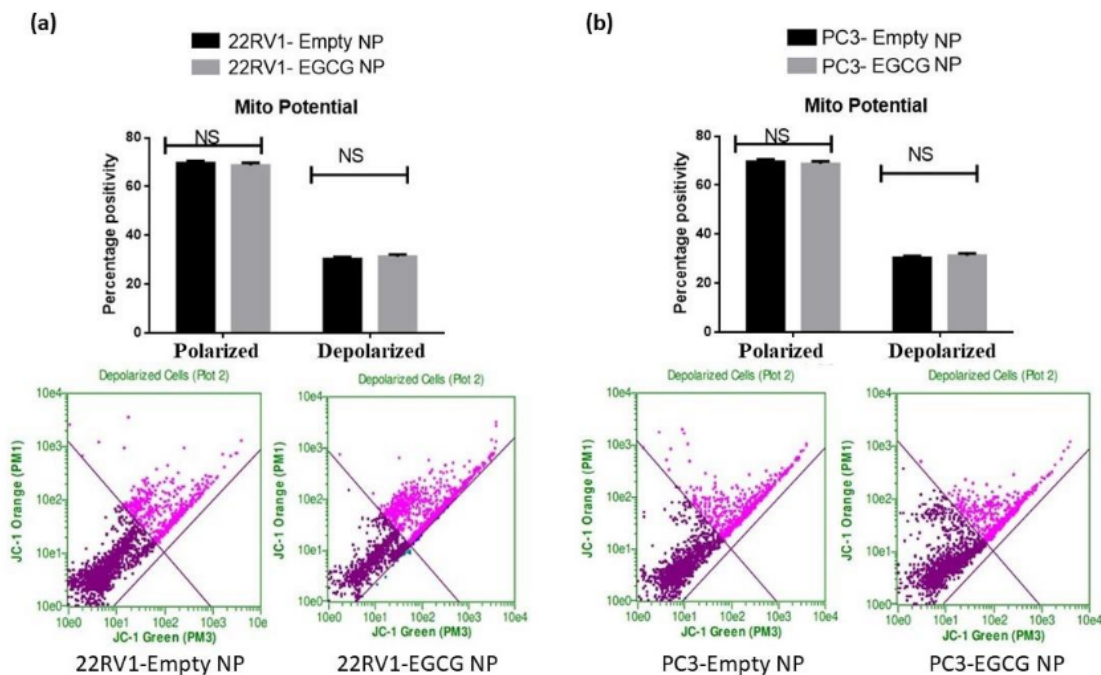
**Figure 6:** EGCG NPs fails to induce depolarization in PCa spheroids. The treated spheroids were mixed with JC-1 dye at the time point's end, and they were then incubated for 30 minutes at 37°C. The manufacturer-provided standardized wavelength for the Guava Flow Cytometer was used to measure the fluorescent intensity. The values are shown as the mean ± SEM (n = 6).

**EGCG treatment promotes apoptosis in PCa cells**

Figure 7 (a, b), upper and lower panels show that there was a highly significant difference between 22Rv1 and PC3 spheroids treated with EGCG in terms of the number of living and apoptotic cells. Moreover, 22Rv1 cells treated with EGCG showed an increase in apoptotic cells of almost 72% (from 10.6% to 38.2%) when compared to control. However, the number of apoptotic cells increased in PC3 spheroids treated with EGCG by 31% (from 26.1% to 38.1%) in comparison to control. These results were expected, as the EGCG has been reported to induce apoptosis in various cancer models (Zhao et al., 2021, Khiewkamrop et al., 2022). However, the EGCG NPs were failed to show a significant change in live and apoptotic cells in 22Rv1 and PC3 spheroids compared to empty NPs.
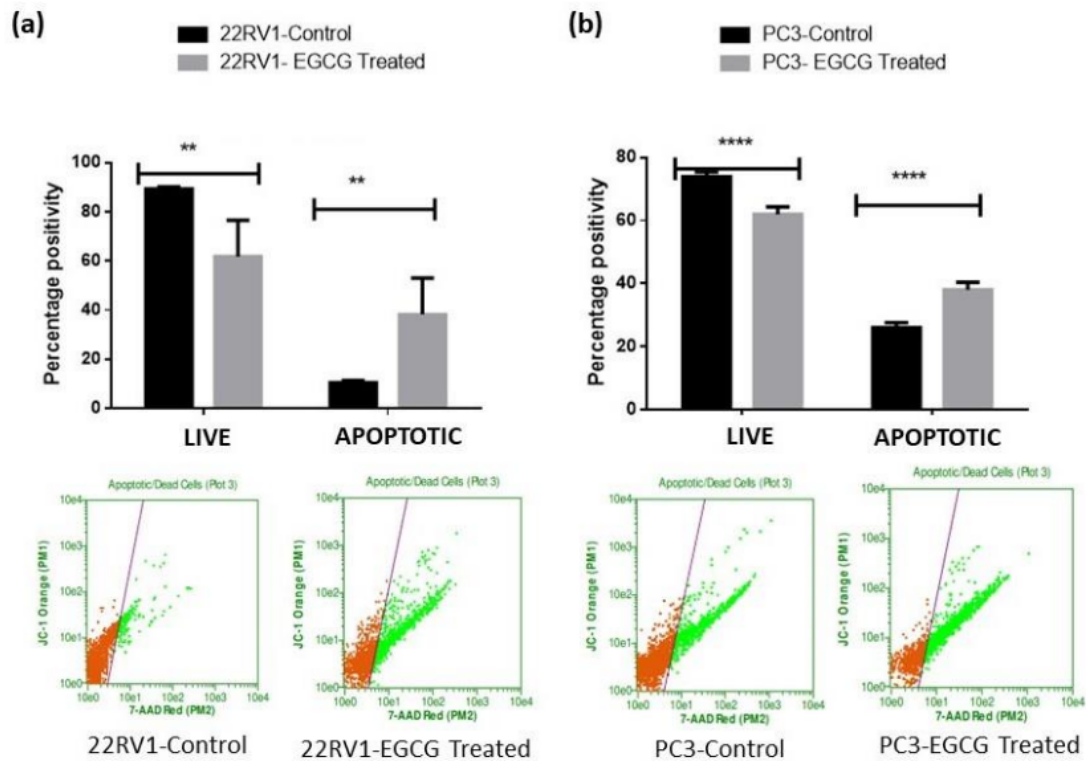
**Figure 7:** EGCG induced apoptosis in PCa spheroids. The treated spheroids received PI dye at the end of the time point, and they were then incubated for 30 minutes at 37°C. Using a Guava Flow Cytometer and a defined wavelength that the manufacturer provided, fluorescent intensity was assessed. The values are shown as the mean ± SEM (n = 6). **P < 0.01 and ***P < 0.001.
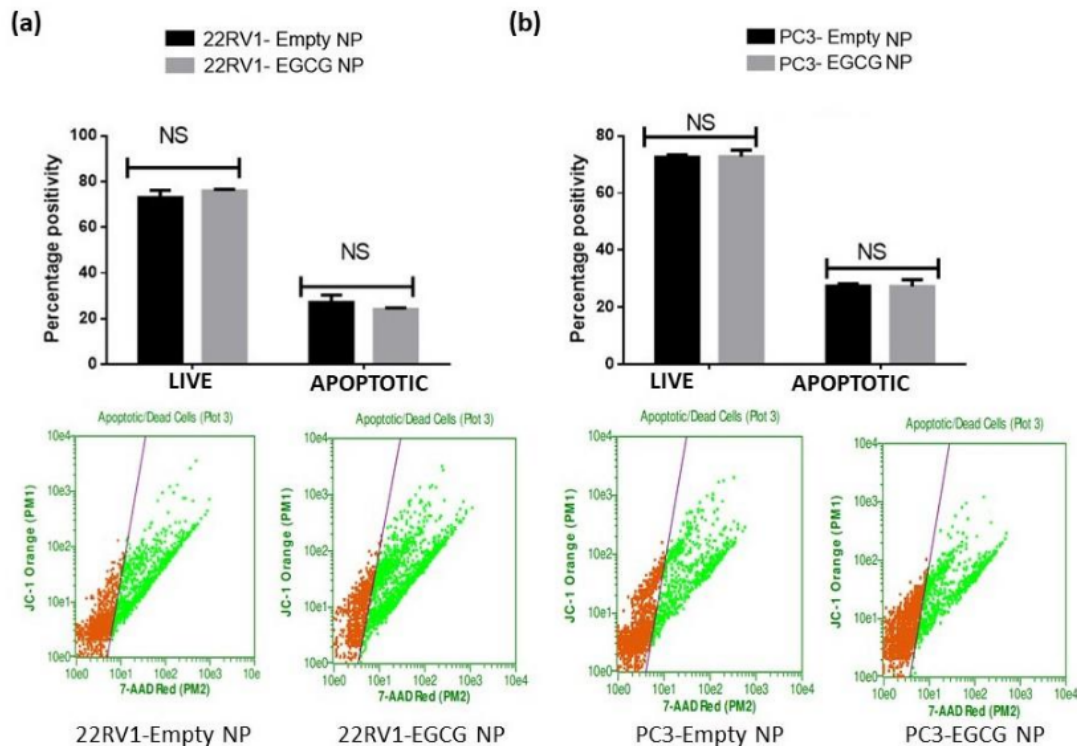
**Figure 8:** EGCG NPs fails to induce apoptosis in PCa spheroids. The treated spheroids received PI dye at the end of the time point, and they were then incubated for 30 minutes at 37°C. Using a Guava Flow Cytometer and a defined wavelength that the manufacturer provided, fluorescent intensity was assessed. The values are shown as the mean ± SEM (n = 6). **P < 0.01 and ***P < 0.001.

**Conclusion**

Overall, our results indicate the anticancer efficacy of EGCG and EGCG NPs in 3D spheroids of PCa cell lines. The spheroid sizes of studied cell lines were significantly reduced after the treatment with EGCG and EGCG NPs. The EGCG and EGCG NPs induced ROS in PC3 and not induced in 22Rv1 possibly suggesting, no role of receptor mediated antigen i.e., PSMA. Surprisingly, we didn't observe any significant changes in mitochondrial membrane potential treated with EGCG or EGCG NP in 22Rv1 and PC3 spheroids. There was significant increase in apoptotic cells in EGCG treated groups. Overall, our results indicate a significant anticancer potential of EGCG alone. In addition, the nanoform version mostly showed better potential compared with EGCG

14

alone. Further, preclinical *in vivo* studies and possible modulation in nanoform are recommended that could verify our *in vitro* data and further enhance its potential for possible usage in clinics.

**Conflict of interests:** None declared

**Acknowledgments:**

## References

Adamczuk, G., E. Humeniuk, M. Iwan, et al., 2021. The Mitochondria-Independent Cytotoxic Effect of Leflunomide on RPMI-8226 Multiple Myeloma Cell Line. Molecules. 26 (18) 5653. https://doi.org/10.3390/molecules26185653

Ahmad, A., M. M. Ansari, R. K. Verma, et al., 2021. Aminocellulose-Grafted Polymeric Nanoparticles for Selective Targeting of CHEK2-Deficient Colorectal Cancer. ACS Appl. Bio Mater. 4 (6) 5324-5335. https://doi.org/10.1021/acsabm.1c00437

Ahmad, A., A. Gupta, M. M. Ansari, et al., 2020. Hyperbranched Polymer-Functionalized Magnetic Nanoparticle-Mediated Hyperthermia and Niclosamide Bimodal Therapy of Colorectal Cancer Cells. ACS Biomater. Sci. Eng. 6 (2) 1102-1111. https://doi.org/10.1021/acsbiomaterials.9b01947

Ahmad, A., F. Khan, R. K. Mishra, et al., 2019. Precision Cancer Nanotherapy: Evolving Role of Multifunctional Nanoparticles for Cancer Active Targeting. J. Med. Chem. 62 (23) 10475-10496. https://doi.org/10.1021/acs.jmedchem.9b00511

Alserihi, R. F., M. R. S. Mohammed, M. Kaleem, et al., 2022. Development of (−)-epigallocatechin-3-gallate-loaded folate receptor-targeted nanoparticles for prostate cancer treatment. Nanotechnology Reviews. 11 (1) 298-311. https://doi.org/10.1515/ntrev-2022-0013

Batra, J. S., K. J. Pienta, M. G. Pomper, et al., 2019. Can the interplay between androgen signaling and PSMA expression be leveraged for theranostic applications? Translational Andrology and Urology. 0 (0) S263-S226S264. https://doi.org/10.21037/tau.2019.03.13

Białkowska, K., P. Komorowski, M. Bryszewska, et al., 2020. Spheroids as a Type of Three-Dimensional Cell Cultures-Examples of Methods of Preparation and the Most Important Application. Int J Mol Sci. 21 (17) E6225. https://doi.org/10.3390/ijms21176225

Bosutti, A., F. Zanconati, G. Grassi, et al., 2016. Epigenetic and miRNAs Dysregulation in Prostate Cancer: The role of Nutraceuticals. Anticancer Agents Med Chem. 16 (11) 1385-1402. https://doi.org/10.2174/1871520616666160425105257

Chen, H., X. Wei, H. Chen, et al., 2019. The study of establishment of an in vivo tumor model by three-dimensional cells culture systems methods and evaluation of antitumor effect of biotin-conjugated pullulan acetate nanoparticles. Artif Cells Nanomed Biotechnol. 47 (1) 123-131. https://doi.org/10.1080/21691401.2018.1544142

Cheng, Z., Z. Zhang, Y. Han, et al., 2020. A review on anti-cancer effect of green tea catechins. Journal of Functional Foods. 74 104172. https://doi.org/10.1016/j.jff.2020.104172

Choi, J. W., S.-H. Bae, I. Y. Kim, et al., 2021. Testing in vitro toxicity of nanoparticles in 3D cell culture with various extracellular matrix scaffold. https://doi.org/10.1101/2021.03.18.436024

Dai, W., C. Ruan, Y. Zhang, et al., 2020. Bioavailability enhancement of EGCG by structural modification and nano-delivery: A review. Journal of Functional Foods. 65 103732. https://doi.org/10.1016/j.jff.2019.103732

El-Didamony, S. E., R. I. Amer and G. H. El-Osaily, 2022. Formulation, characterization and cellular toxicity assessment of a novel bee-venom microsphere in prostate cancer treatment. Sci Rep. 12 (1) 13213. https://doi.org/10.1038/s41598-022-17391-w

Farooqi, A. A., M. Pinheiro, A. Granja, et al., 2020. EGCG Mediated Targeting of Deregulated Signaling Pathways and Non-Coding RNAs in Different Cancers: Focus on JAK/STAT, Wnt/β-Catenin, TGF/SMAD, NOTCH, SHH/GLI, and TRAIL Mediated Signaling Pathways. Cancers. 12 (4) 951. https://doi.org/10.3390/cancers12040951

Ferrari, E., S. Bettuzzi and V. Naponelli, 2022. The Potential of Epigallocatechin Gallate (EGCG) in Targeting Autophagy for Cancer Treatment: A Narrative Review. Int J Mol Sci. 23 (11) 6075. https://doi.org/10.3390/ijms23116075

Gul, S., S. H. Hassan, A. Maryam, et al., 2022. Chemopreventive and Chemosensitizing Effects of Green Tea: An Evidence-based Review. PJZ. 54 (5) https://doi.org/10.17582/journal.pjz/20191021131001

Hundsberger, H., A. Stierschneider, V. Sarne, et al., 2021. Concentration-Dependent Pro- and Antitumor Activities of Quercetin in Human Melanoma Spheroids: Comparative Analysis of 2D and 3D Cell Culture Models. Molecules. 26 (3) 717. https://doi.org/10.3390/molecules26030717

Hung, H.-I., O. J. Klein, S. W. Peterson, et al., 2016. PLGA nanoparticle encapsulation reduces toxicity while retaining the therapeutic efficacy of EtNBS-PDT in vitro. Sci Rep. 6 (1) 33234. https://doi.org/10.1038/srep33234

Ivanova, D., Z. Zhelev, I. Aoki, et al., 2016. Overproduction of reactive oxygen species - obligatory or not for induction of apoptosis by anticancer drugs. Chin J Cancer Res. 28 (4) 383-396. https://doi.org/10.21147/j.issn.1000-9604.2016.04.01

Jabir, N. R., C. K. Firoz, A. Bhushan, et al., 2018. The Use of Azoles Containing Natural Products in Cancer Prevention and Treatment: An Overview. Anticancer Agents Med Chem. 18 (1) 6-14. https://doi.org/10.2174/1871520616666160520112839

Jabir, N. R., M. T. Islam, S. Tabrez, et al., 2018. An insight towards anticancer potential of major coffee constituents. BioFactors. 44 (4) 315-326. https://doi.org/10.1002/biof.1437

Jabir, N. R., S. Tabrez, G. M. Ashraf, et al., 2012. Nanotechnology-based approaches in anticancer research. Int J Nanomedicine. 7 4391-4408. https://doi.org/10.2147/ijn.s33838

Khiewkamrop, P., D. Surangkul, M. Srikummool, et al., 2022. Epigallocatechin gallate triggers apoptosis by suppressing de novo lipogenesis in colorectal carcinoma cells. FEBS Open Bio. 12 (5) 937-958. https://doi.org/10.1002/2211-5463.13391

Lazzari, G., P. Couvreur and S. Mura, 2017. Multicellular tumor spheroids: a relevant 3D model for the in vitro preclinical investigation of polymer nanomedicines. Polym. Chem. 8 (34) 4947-4969. https://doi.org/10.1039/C7PY00559H

Li, H., M. Zhang, X. Wang, et al., 2022. Advancements in the treatment of metastatic hormone-sensitive prostate cancer. Front Oncol. 12 913438. https://doi.org/10.3389/fonc.2022.913438

Li, S., S. Zhao, Y. Guo, et al., 2022. Clinical Efficacy and Potential Mechanisms of Acupoint Stimulation Combined With Chemotherapy in Combating Cancer: A Review and Prospects. Front Oncol. 12

Liu, C., P. Li, Z. Qu, et al., 2019. Advances in the Antagonism of Epigallocatechin-3-gallate in the Treatment of Digestive Tract Tumors. Molecules. 24 (9) E1726. https://doi.org/10.3390/molecules24091726

Lushchak, V. I., 2016. Time-course and intensity-based classifications of oxidative stresses and their potential application in biomedical, comparative and environmental research. Redox Report. 21 (6) 262-270. https://doi.org/10.1080/13510002.2015.1126940

Mazurakova, A., M. Samec, L. Koklesova, et al., 2022. Anti-prostate cancer protection and therapy in the framework of predictive, preventive and personalised medicine — comprehensive effects of phytochemicals in primary, secondary and tertiary care. EPMA Journal. 13 (3) 461-486. https://doi.org/10.1007/s13167-022-00288-z

Michy, T., T. Massias, C. Bernard, et al., 2019. Verteporfin-Loaded Lipid Nanoparticles Improve Ovarian Cancer Photodynamic Therapy In Vitro and In Vivo. Cancers. 11 (11) E1760. https://doi.org/10.3390/cancers11111760

Mittal, S., P. K. Sharma, R. Tiwari, et al., 2017. Impaired lysosomal activity mediated autophagic flux disruption by graphite carbon nanofibers induce apoptosis in human lung epithelial cells through oxidative stress and energetic impairment. Part Fibre Toxicol. 14 (1) 15. https://doi.org/10.1186/s12989-017-0194-4

Oves, M., M. Aslam, M. Rauf, et al., 2018. Antimicrobial and anticancer potential of silver nanoparticles synthesized from trivial Phoenix dactylifera root hair extracts. Materials Science & Engineering C. 89 429-443.

Perez, J. E., I. Nagle and C. Wilhelm, 2021. Magnetic molding of tumor spheroids: emerging model for cancer screening. Biofabrication. 13 (1) 015018. https://doi.org/10.1088/1758-5090/abc670

Picot, F., R. Shams, F. Dallaire, et al., 2022. Image-guided Raman spectroscopy navigation system to improve transperineal prostate cancer detection. Part 1: Raman spectroscopy fiber-optics system and in situ tissue characterization. J Biomed Opt. 27 (9) https://doi.org/10.1117/1.JBO.27.9.095003

Pinto, B., A. C. Henriques, P. M. A. Silva, et al., 2020. Three-Dimensional Spheroids as In Vitro Preclinical Models for Cancer Research. Pharmaceutics. 12 (12) 1186. https://doi.org/10.3390/pharmaceutics12121186

Porporato, P. E., N. Filigheddu, J. M. B.-S. Pedro, et al., 2018. Mitochondrial metabolism and cancer. Cell Res. 28 (3) 265-280. https://doi.org/10.1038/cr.2017.155

Russo, G. L., E. Stampone, C. Cervellera, et al., 2020. Regulation of p27Kip1 and p57Kip2 Functions by Natural Polyphenols. Biomolecules. 10 (9) 1316. https://doi.org/10.3390/biom10091316

Sayegh, N., U. Swami and N. Agarwal, 2022. Recent Advances in the Management of Metastatic Prostate Cancer. JCO Oncology Practice. 18 (1) 45-55. https://doi.org/10.1200/OP.21.00206

Sims, L. B., M. K. Huss, H. B. Frieboes, et al., 2017. Distribution of PLGA-modified nanoparticles in 3D cell culture models of hypo-vascularized tumor tissue. Journal of Nanobiotechnology. 15 (1) 67. https://doi.org/10.1186/s12951-017-0298-x

Sung, H., J. Ferlay, R. L. Siegel, et al., 2021. Global Cancer Statistics 2020: GLOBOCAN Estimates of Incidence and Mortality Worldwide for 36 Cancers in 185 Countries. CA: A Cancer Journal for Clinicians. 71 (3) 209-249. https://doi.org/10.3322/caac.21660

Tabrez, S., M. Priyadarshini, M. Urooj, et al., 2013. Cancer chemoprevention by polyphenols and their potential application as nanomedicine. J Environ Sci Health C Environ Carcinog Ecotoxicol Rev. 31 (1) 67-98. https://doi.org/10.1080/10590501.2013.763577

Zhao, J., A. Blayney, X. Liu, et al., 2021. EGCG binds intrinsically disordered N-terminal domain of p53 and disrupts p53-MDM2 interaction. Nat Commun. 12 (1) 986. https://doi.org/10.1038/s41467-021-21258-5

# RManuscript 23.01.2023.docx

ORIGINALITY REPORT

## 13%
SIMILARITY INDEX

PRIMARY SOURCES

**1**    **www.degruyter.com**
Internet

424 words — **11%**

**2**    Nasimudeen R. Jabir, Md Tabish Rehman, Mohamed F. AlAjmi, Bakrudeen Ali Ahmed, Shams Tabrez. "Prioritization of bioactive compounds envisaging yohimbine as a multi targeted anticancer agent: insight from molecular docking and molecular dynamics simulation", Journal of Biomolecular Structure and Dynamics, 2022
Crossref

29 words — **1%**

**3**    **www.mdpi.com**
Internet

26 words — **1%**

EXCLUDE QUOTES    ON        EXCLUDE SOURCES    < 1%

EXCLUDE BIBLIOGRAPHY    ON        EXCLUDE MATCHES    < 10 WORDS